

# The role of adsorbed hydroxyl species in the electrocatalytic carbon monoxide oxidation reaction on platinum

Anthony R. Kucernak,\*<sup>1</sup>, Gregory J. Offer<sup>a</sup>

Received (in XXX, XXX) 1st January 2007, Accepted 1st January 2007

<sup>5</sup> First published on the web 1st January 2007

DOI: 10.1039/b000000x

The assumption that “OH<sub>ads</sub>” or other oxygen containing species is formed on polycrystalline or nanoparticulate platinum through a fast and reversible process at relatively low potentials is often made. In this paper we discuss the implications of this assumption and the difficulty in reconciling  
10 it with experimental phenomena. We show how presenting chrono-amperometric transients as log-log plots for potentials steps in the presence and absence of an adlayer of carbon monoxide on polycrystalline platinum is particularly useful in understanding the time evolution of the CO oxidation reaction. When using log-log plots a clear power law decay can be observed in the transients both in the presence and absence of an adlayer of carbon monoxide. We explain this as  
15 an extension of current theory, such that the rate determining step in both cases is the formation of a hydrogen bonded water-OH<sub>ads</sub> network, strongly influenced by anions, and that CO<sub>ads</sub> oxidation occurs, at least in part by the diffusion of OH<sub>ads</sub> through this network. We hypothesize that, at low potentials the formation of OH<sub>ads</sub> at active sites is fast and reversible but that transport of OH<sub>ads</sub> away from those sites may be rate limiting. The assumption that overall OH<sub>ads</sub> formation on  
20 platinum is fast and reversible is therefore highly dependent upon the platinum surface and the experimental conditions and it may not be appropriate for polycrystalline surfaces in sulphuric acid. Therefore, although the formation of OH<sub>ads</sub> on platinum in the absence of strongly adsorbing anions on ‘ideal’ surfaces is almost certainly fast and reversible, on realistic fuel cell relevant surfaces under non-ideal conditions this assumption cannot be made, and instead the formation of  
25 an OH<sub>ads</sub> adlayer may be somewhat slow and is associated with the formation of hydrogen bonded water-OH<sub>ads</sub> networks on the surface. We expect this to be a more realistic description for what occurs during CO<sub>ads</sub> oxidation on fuel cell relevant catalysts which are highly heterogeneous and which have a highly defective surface.

---

<sup>1</sup> Department of Chemistry, Imperial College London, United Kingdom Fax: 44 20 75945804; Tel: 44 20 75945831; E-mail: a.kucernak@imperial.ac.uk

## Introduction

The formation of oxides on platinum surfaces at high potentials is relatively well studied yet contentious. The role of the species typically called “OH<sub>ads</sub>” in the surface catalysis of platinum catalysts is crucial in understanding a large number of reactions, of which the most common example is the carbon monoxide oxidation reaction (COOR). The nature of this species is somewhat controversial, although Anderson has recently shown through theoretical ab initio charge self-consistent methods that OH<sub>ads</sub> should form on a Pt surface at a potential of about 0.6 V. Several investigators claim that OH<sub>ads</sub> is the species responsible for reacting with adsorbed CO<sub>ads</sub>, and that this is a chemical Langmuir-Hinshelwood (L-H) reaction<sup>1-7</sup>. The lowest potentials at which the COOR has been reported is 150 mV for carbon supported platinum<sup>8</sup>, 200 mV for a porous platinum electrode<sup>9</sup> and for polycrystalline platinum<sup>10</sup>, and 300 mV for a Pt(111) electrode<sup>11</sup>, and it has been shown that there is a relationship between the number of defects and the activity of the surface<sup>12</sup>. As a result some have suggested that if the L-H mechanism is operative, then the CO<sub>ads</sub> oxidation activity observed in the hydrogen region implies that OH<sub>ads</sub> must be present at these potentials<sup>1-9, 11, 13</sup>. Indeed, it has been shown that the formation of OH<sub>ads</sub> can be demonstrated on platinum in acidic solutions at potentials as low as 400 mV<sup>14-17</sup>. Where do the oxygen containing species come from? The role of step edges and defect sites in OH<sub>ads</sub> formation is often invoked to explain the early onset of CO<sub>ads</sub> oxidation<sup>1, 3, 4, 6, 11, 12</sup>. For a thorough review of this subject the reader is referred to Markovic et al.<sup>7</sup>.

In contrast, a number of studies of the formation of oxides on platinum assume that the onset of formation of oxygen containing species on polycrystalline or nanostructured Pt does not occur until above 700 mV<sup>18-23</sup> and some have even claimed that it has been ‘unambiguously proven’<sup>21</sup> that the initial oxide growth on Pt leads directly to the formation of PtO<sup>20, 21, 23</sup>, contrary to others who suggest it is via the formation of OH<sub>ads</sub><sup>22</sup>. This is despite the fact that it is known that the formation of OH<sub>ads</sub> on Pt(111) and Pt(100) takes place in wide potential regions positive to the potential of zero charge of these surfaces but significantly less positive than the threshold for the formation of the surface oxide phases<sup>24</sup>. Therefore, there seems to be a problem in rationalising between the need for oxygen containing species on polycrystalline or nanostructured Pt at low potentials (otherwise known reactions could not proceed), and the belief that the oxide formation region on these Pt surfaces only begins at 700mV, and even the belief that OH<sub>ads</sub> is never present. For a complete discussion of this subject up to the mid 90’s the reader is referred to Conway<sup>25</sup>.

In this paper we discuss the merit of the various arguments both supporting and opposing the formation of OH<sub>ads</sub> at such low potentials, and in the process challenge the assumption that the so called double layer region in the typical platinum cyclic voltammogram does not contain any faradaic processes. For clarity we will refer to adlayers of OH<sub>ads</sub> as hydroxyl layers, and adlayers of O<sub>ads</sub> as oxide layers.

In this paper we present experimental investigations conducted on polycrystalline Pt primarily using potential step

techniques as recommended by McCallum and Pletcher<sup>26</sup> over a 300 mV potential window, larger than typically used for these sorts of experiments. Furthermore, we limit the studies to polycrystalline Pt and not ideal single crystal electrodes; this is a deliberate choice, and represents the decision to move towards realistic catalysts such as carbon supported Pt and PtRu; which will be presented in a further paper, rather than single crystal electrodes which may still contain some defects<sup>27</sup>. This is because the work was intended as an investigation into catalyst systems for fuel cell applications, and as such real catalysts are of more practical interest.

## Oxide versus hydroxyl formation

In order to understand the role of hydroxyl in the surface catalysis of Pt it is necessary to resolve the differences between hydroxyl and oxide and separate hydroxyl formation from oxide formation. The two are often considered together and the majority of studies aimed at resolving hydroxyl/oxide formation on Pt have been conducted at potentials within the ‘traditional’ oxide growth region (0.8 to 1.4 V)<sup>18-23</sup>, ignoring the region at lower potentials. This is perhaps a result of the seminal work by Conway’s group<sup>22</sup> in the 70’s which has contributed greatly to the development of understanding of hydroxyl/oxide growth formation on Pt. The fundamental assumption made in the Conway paper is that there are no oxides or hydroxyls present on the Pt surface below 0.7-0.8 V (see Fig. 1. ref<sup>22</sup>) and that any charges passed between 0.4 V and 0.7-0.8 V are due to double layer charging alone. It is perhaps because of this underlying assumption that the analysis of Pt oxide growth has often been limited to potentials above 0.8 V<sup>18-23</sup>. In the paper by Conway et al.<sup>22</sup> the typical two anodic peaks and shoulder in the Pt i-V profile are considered as occurring before a monolayer of hydroxyl has been formed, even at a single crystal surface, and based on this assumption they showed that the hydroxyl monolayer became irreversibly adsorbed above about 0.95 V, with a coverage of approximately 0.25, which was well below the monolayer limit of one hydroxyl per Pt, which occurred at 1.1 V. However, it is unlikely that the formation of an adsorbed layer of hydroxyl could be anything other than reversible unless it results in a reorganisation of the Pt surface with migration of hydroxyl into the bulk, as suggested by Conway et al. (see Fig. 21. ref<sup>22</sup>), which does not appear to be supported by any further evidence in their paper. For a comprehensive review of oxide formation up to the mid 90’s the reader is referred to Conway and references therein<sup>25</sup>.

More recently, an ac voltammetry study of Pt hydroxyl/oxide growth during potential sweep experiments by Harrington et al.<sup>20</sup> disagreed with this proposed mechanism. They showed that in the formation of Pt oxide films an initial step involving electrosorption of hydroxyl species is unlikely, and that the rate-determining step in the growth of the oxide film is the event in which the Pt moves from its metal lattice site to become a Pt(II) species; when the oxide begins to migrate into the bulk Pt. They stated that this is a two electron oxidation of a Pt atom. They did note that the oxide growth region is reversible if the reversal potential is less than 0.8 V, but

disagreed that this could be attributed to reversible hydroxyl adsorption occurring before the Pt atom becomes part of the growing oxide film (the turnover process). They showed that fast adsorption of hydroxyl before a slow rds would lead to features which were not seen in the ac impedance spectra. They also suggested that it is incorrect to attribute the three features seen in the oxide region to three different superlattice structures of hydroxyl species<sup>28</sup>. Instead, they associated these peaks to the slow formation of oxide depending upon the surface structure. Fundamentally they argued that the formation of a hydroxyl species is not implicated in oxide formation above 0.8V(RHE)<sup>†</sup>, and so the hydroxyl species cannot be present. As a result of this paper some have even claimed that this has been ‘unambiguously proven’<sup>21</sup> and that the initial oxide growth on Pt leads directly to the formation of PtO<sup>20, 21, 23</sup>.

In addition all the papers upon which Alsabet et al. based their supporting arguments were done at potentials above 0.8 V<sup>18-23</sup> and as shall be demonstrated in this paper this potential may already be near the saturation coverage of hydroxyl species and the onset of irreversibility could well be closer to the onset of formation a monolayer of oxide and not hydroxyl. Therefore if the formation of hydroxyl is sufficiently fast at these potentials, then the caution that Harrington et al.<sup>20</sup> added to their paper, that their observed transfer coefficient could also be consistent with a slow one-electron transfer as the rate determining step followed by a further electron transfer in a faster step, may well need to be considered.

### Hydroxyl formation

Moving from the arguments against hydroxyl formation found in the literature to arguments for hydroxyl formation found in the literature it is useful to start with a discussion of the potential of zero charge (pzc). This is used by electrochemists to describe the lowest potential at which anions begin to predominate over cations on a surface. Bockris and Argade<sup>17</sup> reviewed the determination of the pzc on solid metals, including platinum, gold, silver, and nickel in 1969. They assessed the pzc, both experimentally and by comparing a large number of authors using 3 different techniques; adsorption in the double layer of a neutral organic compound as a function of the concentration of the supporting electrolyte; double-layer capacitance as a function of potential; and static friction between surfaces in solution. The pzc for platinum was found to be 560 mV at a pH of zero, and 67 mV lower for each unit increase in pH.

In 1996 Iwasita and Xia<sup>29</sup> then reported the potential of zero charge (pzc) on platinum(111) as being close to 350 mV vs RHE in 0.1 mol dm<sup>-3</sup> perchloric acid. In particular they discussed the importance of adsorbed water in electrocatalytic reactions. They described a growing interaction between the 3a<sub>1</sub> orbitals of water with d orbitals of the metal between 500 mV and 900 mV, consistent with a molecular state preceding dissociation, specifically partial dissociation to form adsorbed hydroxyl ions. They stated that co-adsorbed OH<sup>-</sup> ions from

water dissociation probably start being formed at 500 mV, and the saturation equilibrium between adsorbed water and OH<sup>-</sup> is probably reached at ca. 900 mV. Climent et al. also showed that complete monolayers of OH<sub>ads</sub> are achieved on a Pt(111) surface in perchloric acid above 800mV<sup>24</sup>, calculated by integrating the once controversial ‘butterfly’ features first reported by Clavilier (see fig. 2 ref<sup>30</sup>). However Climent et al. assumed that the ‘butterfly’ features are the formation of OH<sub>ads</sub>, whereas Clavilier originally assumed that they were the desorption of H<sub>ads</sub>. That they are OH<sub>ads</sub> does not seem to be in dispute<sup>31, 32</sup>, however, Clavilier also reported features between 300 mV and 500 mV in sulphuric acid (see fig. 1 ref<sup>30</sup>) and assumed that they were the same as those seen between 600 mV and 800 mV in perchloric acid for Pt(111), which combined with the logic of Climent et al. would make a complete monolayer of OH<sub>ads</sub> achievable on Pt(111) in sulphuric acid above 500 mV. This seems extremely unlikely. More recently, these features in sulphuric acid have been explained as anion adsorption<sup>33</sup>. Other authors have not seen the corresponding ‘butterfly’ features for Pt(111) in sulphuric acid<sup>34</sup>, confusing matters entirely, however the cyclic voltammograms appear very dissimilar, suggesting that the surfaces were not identical, and perhaps not as ‘ideal’ as hoped for. However, if the surfaces were not ideal, perhaps with greater defects, and more like polycrystalline Pt, why do these features disappear, and for polycrystalline Pt in both perchloric and sulphuric acid? This does not seem to have been adequately explained. If the peaks in perchloric acid were OH<sub>ads</sub> formation and OH<sub>ads</sub> formation is fast and reversible as is often assumed, then why do they not occur on polycrystalline Pt where there are more active sites?. And in sulphuric acid if they are anion adsorption, again why are they not seen for polycrystalline Pt, and where are the OH<sub>ads</sub> formation peaks? Therefore it does not appear clear at all where when and how OH<sub>ads</sub> formation occurs on polycrystalline Pt in acidic solutions, whether it is fast and reversible, or how the surface orientation or anions affect it, we only know that it must occur otherwise known reactions could not happen.

Even more worrying is that the assumption that the charge associated with a monolayer of adsorbed hydrogen on Pt of 210 μC cm<sup>-2</sup><sup>34</sup> is implicitly based upon the assumption that there is only H<sub>ads</sub> present within the hydrogen region, therefore any overlap with a hydroxyl formation region could have significant implications on this value, and the practice of integrating the hydrogen region and comparing to this value to estimate the electrochemical surface area of different surfaces. However, above potentials of about 800 mV platinum voltammograms appear to become more comparable with similar features being seen for different surfaces, and this would appear to fit very closely with the onset of irreversibility in the oxide formation region described earlier<sup>20, 22</sup>. This is also in broadly the correct region of potentials at which the oxygen reduction reaction (ORR) becomes significantly inhibited, which has been explained as the presence of a complete monolayer of OH<sub>ads</sub> (see Fig. 7 in<sup>35</sup>). Although the onset of inhibition of the ORR in this example<sup>35</sup> does not begin to occur until 700 mV this does not necessarily

<sup>†</sup> Unless otherwise stated, all potentials in this paper are referenced to the RHE electrode

mean that there is no hydroxyl present below these potentials. Indeed, OH<sub>ads</sub> may be an intermediate in the oxygen reduction reaction. If a parallel can be drawn with the poisoning of the HOR by CO<sub>ads</sub> where it is possible to detect appreciable HOR currents at very high CO<sub>ads</sub> coverages; with 90% of the diffusion limited current possible at relative coverages as high as 0.95<sup>8</sup>, then we suggest it is reasonable to suppose that significant coverages of hydroxyl species could exist below 700 mV.

More recently an acknowledgement of the limitations of the pzc when characterising inhomogeneous surfaces has become apparent and the introduction of the potential of zero total charge (pztc) has become more widespread. For a useful review of the concept of the pztc and the methods used in its determination the reader is referred to Attard et al.<sup>36</sup> Using the CO-displacement method first described by Climent et al.<sup>37</sup> Mayrhofer et al.<sup>35</sup> described the potential of zero total charge (pztc) for a number of platinum surfaces. The pztc of polycrystalline Pt was shown to be ~285 mV, changing to 245 mV for a 1nm Pt particle<sup>35</sup>, and they suggested it is therefore conceivable that hydroxyl species could be present and stable around these potentials on active sites and defects. Further papers by Mayrhofer et al.<sup>38, 39</sup> highlighting the role of defects in the particle size effect of Pt nanoparticles also suggest that the catalytic activity for CO<sub>ads</sub> oxidation is predominantly influenced by the ability of the Pt surface to dissociate water and form OH<sub>ads</sub> on defect sites, with the onset of CO<sub>ads</sub> oxidation seen at approximately 250 mV, suggesting the formation of OH<sub>ads</sub> at 250 mV.

We repeated these experiments for our system and measured a potential of zero total charge of 234 ±5 mV for polycrystalline platinum in 0.5 mol dm<sup>-3</sup> sulphuric acid, which is less than the value of ~285 mV reported by Mayrhofer et al. for polycrystalline Pt in 0.1 mol dm<sup>-3</sup> perchloric acid solution<sup>35</sup>. This is not surprising considering the increased effect of anion adsorption in sulphuric acid compared to perchloric acid.

These results seem to lend a certain amount of support to the ideas presented by Burke<sup>1</sup> in 1994 in a paper which discussed the formation of pre-monolayer hydroxyl species on noble metals, including platinum, and their role in electrocatalysis. Burke suggested that pre-monolayer oxidation of platinum in acid solution, if similar to that on gold, should yield two regions of hydroxyl species formation commencing at 200 mV and 400 mV, in contrast to the generally regarded onset of monolayer oxide formation on platinum in acid above 800 mV. Burke attributed the small middle peak seen in the hydrogen region at 200 mV on Pt in very clean conditions to the formation of hydroxyl species. He suggested that the ability of Pt to oxidise adsorbed CO<sub>ads</sub> at potentials as low as 200 mV<sup>40</sup> and to achieve diffusion limited dissolved CO oxidation at 470 mV<sup>41</sup>; for which no explanation for the facile oxygen transfer capability of the platinum at such low potentials was provided by the authors, supports the formation of hydroxyl species at these potentials, noting that active sites are likely to be important. Perhaps the most controversial claim in this paper was the interpretation of the middle peak seen in the hydrogen desorption region as the formation of a hydroxyl species and not removal of under potential deposited

hydrogen. It is clear that attribution of the COOR at such low potentials to a L-H mechanism implicitly acknowledges the presence of adsorbed hydroxyl species at these potentials. Hence it would appear that Burke's suggestions should be considered as a plausible explanation for the ability of Pt to promote the COOR at such low potentials.

#### Carbon monoxide oxidation

An important aspect of the COOR is the marked effect of the potential at which the CO is adsorbed<sup>40</sup>. CO adsorbed on platinum at potentials which fall in the hydrogen adsorption region show an early onset and a peak potential shifted to lower values compared to electrodes for which CO adsorption occurs in the double layer region. The early onset is exhibited in potential sweep experiments by both a pre-peak and a lower peak potential of the main oxidation peak compared to adlayers prepared in the double layer region.

Currently the most popular theory to explain the early onset of CO<sub>ads</sub> oxidation for CO adlayers on platinum at room temperature prepared in the potential region at which adsorbed hydrogen is present (<350 mV), is that during CO adsorption most, but not all, H<sub>ads</sub> is displaced<sup>9, 42-47</sup>. Oxidation of this remaining H<sub>ads</sub> produces CO-free sites which promote the early onset of CO<sub>ads</sub> oxidation<sup>9, 42-47</sup>. This seems remarkably similar to the approach offered by Burke et al.<sup>48</sup>. These CO free regions then allow the adsorption and/or formation of oxygen containing species, which react with the CO<sub>ads</sub> to form CO<sub>2</sub>. The species involved in the reaction with CO<sub>ads</sub> is generally regarded to be OH<sub>ads</sub> formed by the dissociation of adsorbed water<sup>1, 6, 15-17, 29, 35, 48-50</sup> and L-H kinetics are often assumed<sup>2, 12, 51-55</sup>.

An interesting alternative theory has been proposed by Markovic et al.<sup>11</sup> who explained the early onset of CO<sub>ads</sub> oxidation for adlayers prepared below 150 mV in terms of a weakly adsorbed adlayer (different from individual weakly adsorbed CO<sub>ads</sub> species). They suggest that the more compressed CO<sub>ads</sub> adlayers are less strongly adsorbed because of increased lateral repulsive interactions, and that this reduced adsorption enthalpy enables some OH<sub>ads</sub> to be nucleated at potentials above 150 mV oxidising some CO<sub>ads</sub>. The adlayer then undergoes a relaxation process converting the surface to a less compressed more strongly adsorbed adlayer, and that this more strongly adsorbed adlayer is resistant to OH<sub>ads</sub> nucleation. They report that on Pt(111) this process will completely convert the weakly adsorbed adlayer to the strongly adsorbed adlayer above 250 mV, and they present evidence for the relaxation process on Pt(111) by conducting CO<sub>ads</sub> oxidation stripping voltammetry in the presence of H<sub>2</sub>-saturated solution, and observing a decay in the hydrogen oxidation reaction (HOR) current after either reversing the potential or stopping the CO<sub>ads</sub> oxidation process by potential step before completion. This mechanism could plausibly occur via the free site hopping model of CO diffusion, which showed an exponential increase in CO diffusion with decreasing coverage<sup>56</sup>. It should be noted that the theory proposed by Markovic et al.<sup>11</sup> did not exclude the possibility of co-adsorbed hydrogen and both could occur simultaneously.

Markovic et al. discussed the pH dependence of the CO oxidation reaction in alkaline solutions<sup>7</sup>, and attribute this variation to the “pH dependent” adsorption of OH<sub>ads</sub> at defect/step sites. Although the statement was made with regard to alkaline solutions, we propose in this paper that a similar argument can be applied in acidic solutions; with a slower rate caused by the lower pH. The implications of this on the argument for the presence of hydroxyl in platinum electrocatalysis cannot be underestimated. In this paper we discuss how the role of hydroxyl and its formation at low potentials is extremely important in understanding the COOR mechanism. In addition, the increased role of anions in acidic solutions is also discussed, with implications for fuel cell operation, where anion adsorption is expected to be less relevant due to the fixed nature of the anions in the solid polymer electrolyte.

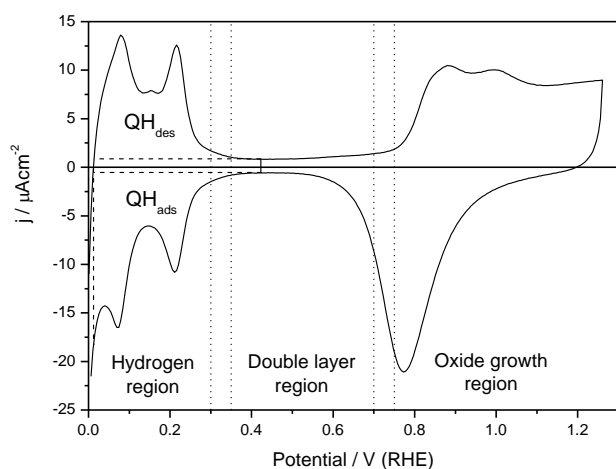


**Figure 1.** Typical cyclic voltammogram of a clean polycrystalline Pt electrode in N<sub>2</sub>-saturated 0.5 mol dm<sup>-3</sup> H<sub>2</sub>SO<sub>4</sub> at a sweep rate of 50 mVs<sup>-1</sup>

## Experimental

The working electrodes used in this study were polycrystalline 125 μm diameter platinum microelectrodes sheathed in glass (3 mm diameter). These were positioned in an impinging jet flow cell configuration<sup>57</sup> as described previously<sup>58, 59</sup> with modifications to ensure uniform access similar to those described by Melville et al.<sup>60</sup>. With this setup it is possible to change the electrolyte bathing the electrode (e.g. CO saturated H<sub>2</sub>SO<sub>4</sub> switching to H<sub>2</sub> saturated H<sub>2</sub>SO<sub>4</sub>) within 200ms. The configuration ensured forced convection at the exposed electrode and the boundary layer thickness was estimated to be ~10 μm based on the limiting current for hydrogen oxidation in the absence of CO (and therefore any diffusion through solution is extremely fast). Saturated CO<sub>ads</sub> adlayers were prepared by exposure of the electrode to CO-saturated 0.5 mol dm<sup>-3</sup> H<sub>2</sub>SO<sub>4</sub> at an admission potential of 50 mV and an admission time of 10s (which because of the strong convection is easily sufficient to ensure a saturated adlayer). Partial adlayers were produced either by exposing the electrode to CO for a much shorter time, 0.1-2s (partial admission), or by taking a CO saturated electrode and pulsing the potential to 800 mV for a defined period (<1s) before

returning it to the admission potential. In both cases, the coverage was calculated by measuring the charge required to remove the remaining CO<sub>ads</sub> in N<sub>2</sub> saturated electrolyte whilst at the same time correcting for double layer and anion adsorption effects<sup>59</sup>. Coverages are reported as a fraction of the saturated CO<sub>ads</sub> adlayer produced under identical conditions. The coverage of the saturated CO<sub>ads</sub> adlayer relative to the H<sub>upd</sub> layer was calculated to be 0.676 with a standard deviation of 1.2% over 5 experiments; assuming a charge density of 210 μC cm<sup>-2</sup> for a monolayer of adsorbed hydrogen<sup>34</sup>. This is in good agreement with similar experiments in the literature for Pt(111) electrodes, for which the maximum coverage in CO-free 0.1 mol dm<sup>-3</sup> H<sub>2</sub>SO<sub>4</sub> was shown to be 0.68<sup>42</sup>. During CO<sub>ads</sub> oxidation experiments it is also important to correct for any residual oxygen reduction<sup>59</sup>.

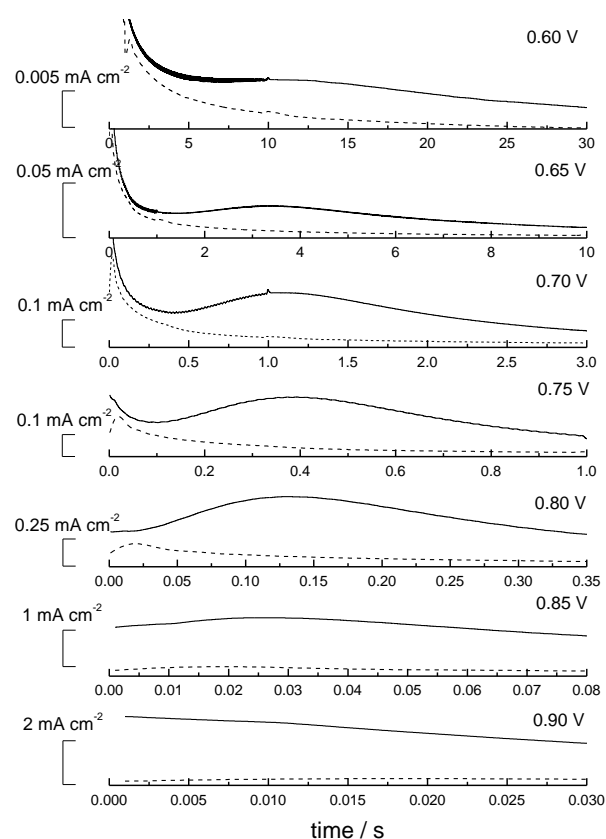


**Figure 2.** Chrono-amperometric transients at potentials from 600 mV to 900 mV for the stripping of saturated CO<sub>ads</sub> adlayers in CO-free 0.5 mol dm<sup>-3</sup> H<sub>2</sub>SO<sub>4</sub> prepared by adsorption of CO at admission potentials of 50 mV, and an admission time of 10 s (—); Same transient in the absence of CO (- - - -).

We therefore took stringent measures to exclude oxygen from these experiments, and measured a background oxygen concentration in the electrolyte of 4.5×10<sup>-8</sup> mol dm<sup>-3</sup>. An example cyclic voltammogram obtainable under these conditions is shown in Figure 1.

## Results

**70 Investigating the oxidation of complete adlayers**

The use of chrono-amperometry to investigate the oxidation of saturated  $\text{CO}_{\text{ads}}$  adlayers formed in the hydrogen region at potentials in the range 0.60-0.90V is shown in Figure 2. Also shown in this diagram are the transients in the absence of any CO. In order to capture the “peak” of the CO oxidation transient, it is necessary to vary the time and current axes by about three orders of magnitude for this 300 mV change in oxidation potential. Although the peaks look similar to each other, it is in no way clear that the same mechanism is operating throughout this entire potential range.

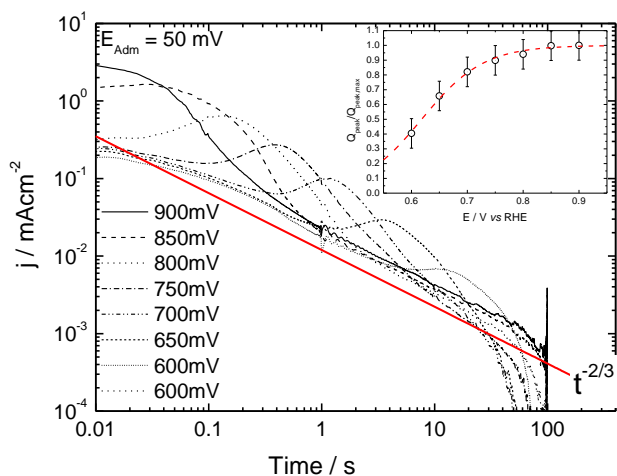


**Figure 3.** Chrono-amperometric transients at potentials from 600 mV to 900 mV for the stripping of saturated  $\text{CO}_{\text{ads}}$  adlayers prepared by adsorption of CO at admission potentials of 50 mV, and an admission time of 10 s. A  $t^{-2/3}$  curve is overlaid. Inset: Relative charge under the peak utilising the  $t^{-2/3}$  curve as a background curve. The charge obtained at the highest potential (0.9V) was used to ratio the charges. The dashed line is a sigmoidal fit to the data constrained between  $Q_{\text{min}}=0$  and  $Q_{\text{max}}=1$ .

When comparing transients performed over such a large potential range (300mV) we found that the most useful way to present the data was as a log-log plot, which enabled comparisons to be made between experiments lasting less than a second to over a hundred seconds, Figure 3. In this case there is a clear progression in the position of peaks, and peak shape appears relatively constant. As the potential is decreased, the peak moves to longer time and smaller current. It is worthwhile pointing out that we are plotting current densities in these diagrams, and a current density of  $10^{-3}$  mA  $\text{cm}^{-2}$  is equivalent to a measured current of  $\sim 0.1$  nA, approaching the limit of what we can measure in these experiments. The non-linearity of the curves between currents of  $10^{-3}$ - $10^{-4}$  mA  $\text{cm}^{-2}$  is probably due to slight errors in current offset ( $\sim 10$ pA or so) and the presence of a small amount of adventitious oxygen providing a small cathodic current. The chrono-amperometric transients for the electrochemical oxidation of  $\text{CO}_{\text{ads}}$  in CO-free  $0.5 \text{ mol dm}^{-3}$   $\text{H}_2\text{SO}_4$  are shown in Figure 3, for which a clear  $\text{CO}_{\text{ads}}$  oxidation peak can be seen for the potential range 600-900 mV, which is overlaid onto a decay which appears to follow a power law with an exponent of  $\sim -2/3$ . Such a power law dependence may be suggestive of a diffusion process. By extrapolating the position and current of the  $\text{CO}_{\text{ads}}$  oxidation peak it is reasonable to assume that we should see peaks below 600 mV

if the experiments had been carried out for a long enough periods of time, and if experimental noise limits had not been reached. In a linear-linear plot of the type shown in Figure 2 it may be quite difficult to distinguish peaks at low potential. When discussing the chrono-amperometric electrochemical oxidation of  $\text{CO}_{\text{ads}}$ , most workers fail to make a comparison to the transient obtained in the absence of any  $\text{CO}_{\text{ads}}$  – the assumption being that these background transients can be either ignored, or subtracted out.

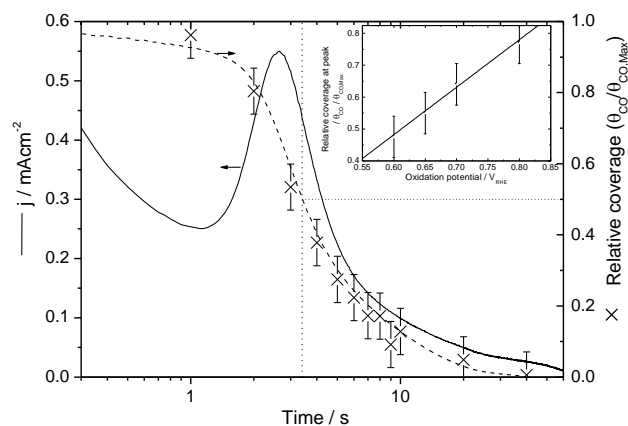


**Figure 4.** Chrono-amperometric transient of a polycrystalline Pt electrode at a potential of 700 mV in  $\text{N}_2$ -saturated  $0.5 \text{ mol dm}^{-3}$   $\text{H}_2\text{SO}_4$  for the stripping of a saturated  $\text{CO}_{\text{ads}}$  adlayer prepared by adsorption of CO at an admission potential of 50 mV and an admission time of 10 s. Relative coverages for  $\text{CO}_{\text{ads}}$  adlayers prepared under identical conditions using partial oxidation are shown (O) with the axis on the right, and fitted with a sigmoidal function for guidance only (dashed line). Inset: Relative coverages calculated from partial oxidation experiments of the peak in the chrono-amperometric transients for the data in the main plot.

Furthermore, many workers subtract out or truncate the initial current decay seen at short times ( $< 1$  s) during the chrono-amperometric oxidation of  $\text{CO}_{\text{ads}}$ , ascribing that initial decay to double layer charging or other background processes. Although a significant amount of initial charge is associated with double layer charging and similar such processes, it is still misleading to remove this information when presenting data. This point is further illustrated by the plot inset into Figure 3. In this figure, the relative integrated charge under the peaks versus oxidation potential are plotted. As a background curve, a transient with a  $t^{-2/3}$  dependence was fit to the current transient before and after the peak, and the excess charge integrated. It can be seen that as the CO oxidation potential is decreased, the charge under the peaks decrease. Indeed, at 0.6 V, the CO oxidation “peak” contains less than 40% of the charge under the CO oxidation peak at 0.9 V. Cyclic voltammetry in our experiments confirms that all of the CO is oxidised during the chonoamperometry, hence especially at lower potentials significant amounts of CO oxidation must occur within the initial transient. Care must be taken in directly relating this charge to CO coverage, as it also contains a component associated with anion adsorption and double layer charging.

A more accurate approach to assess the amount of CO as a function of potential is to halt the oxidation process a certain

length of time into the reaction and then (in a separate experiment) electrochemically strip the remaining adsorbed CO from the surface. We have developed this approach in order to assess the CO coverage as a function of time during the CO oxidation reaction. In this approach, we make corrections for changes in double layer capacitance and anion adsorption to produce a more accurate measure of CO coverage<sup>59</sup>. Provided in Figure 4 is a plot of the CO oxidation transient seen at 0.70 V along with the measured CO coverage as a function of time.

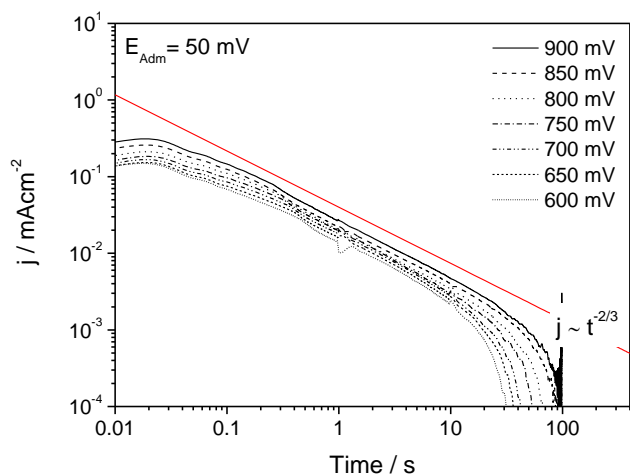


**Figure 5.** Chrono-amperometric transients at potentials of 0.6 V to 0.9 V at 0.05V increments after stepping from a potential of 0.1 V. A  $t^{-2/3}$  curve is overlaid.

Each coverage data point corresponds to a single experiment. The coverages are ratioed to the maximum CO coverage (0.676) seen for this surface. Inset into the diagram are the relative CO coverage at the peak current as a function of oxidation potential. There appears to be an almost linear decrease of the CO coverage at the peak as the potential is reduced. We interpret this to be due to a corresponding increase in CO oxidation in the transient before the peak – i.e. confirmation of the results provided inset to Figure 3.

In Figure 5 we provide Log-Log plots of the current transients of the platinum electrodes in  $N_2$ -saturated 0.5 mol  $dm^{-3}$   $H_2SO_4$ . It is clear that the transients show the same power law decay as seen for the CO oxidation transients with order  $\sim -2/3$ , and that at very low currents there is a downward curve probably due to small levels of adventitious oxygen or a slight instrumental offset current as mentioned above.

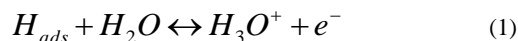
### Transients in the absence of $CO_{ads}$

In properly understanding the  $CO_{ads}$  oxidation process, it is useful to first understand what happens in the absence of any  $CO_{ads}$ . The chrono-amperometric transients for a clean Pt surface in the absence of any  $CO_{ads}$  are shown in Figure 5.

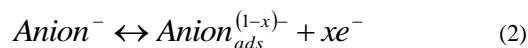
By presenting the transients as a log-log plot it can be seen that there is a decay which appears to follow a power law with an exponent similar to  $-2/3$ , which appears to be identical to that seen in the presence of  $CO_{ads}$ . At longer times, the current deviates from this line and becomes very small or negative, explained by the small amount of residual  $O_2$  in the cell, or a

slight offset current ( $\sim 10$  pA) in the current-to-voltage stage of the potentiostat.

After double layer charging, the transient may be due to one of three different reactions. Firstly, the oxidation of any adsorbed hydrogen, which is considered to be a very fast reaction:



Secondly, anion adsorption, which is generally considered to be a fast process on precious metals<sup>61</sup>:



And thirdly, the oxidation of water to produce an adsorbed hydroxyl species:



The formation of  $OH_{ads}$  is usually considered to be fast and reversible based on the symmetry of the peaks on single crystal platinum. Hence, it does not appear possible that any of the above reactions could be occurring over the timescales needed to be the reason for the power law decay seen in Figure 3 and Figure 5. We are therefore left with the conclusion that either a fourth process is occurring, or that there is something happening which we have not considered. Assuming that there is no fourth reaction, and that the equation 1 is indeed fast, a possible explanation is that the second or third reaction cannot be considered separate from each other. Indeed, for Pt(111) it has been suggested that  $CO_{ads}$  oxidation is accompanied by the adsorption of anions from the supporting electrolyte which affect the adsorption of  $OH$  as well as the mobility of co-adsorbed  $CO$ <sup>62</sup>, and for platinum nanoparticles that the competitive adsorption of bisulfate anions and the existence of irregularities on the platinum surface which may serve as the active centers for  $OH_{ads}$  formation, all play a crucial role in understanding the  $CO_{ads}$  oxidation reaction<sup>39</sup>. Therefore in the absence of  $CO_{ads}$  we could expect a change in potential to give rise to noticeable currents caused by a perturbation of the equilibrium between the competitive adsorption of  $OH_{ads}$  and bisulfate anions and it is conceivable that this could occur over extended timescales.

Therefore, if the third reaction, the formation of hydroxyl species, is the reason for the decay seen in the transients both in the presence and absence of  $CO_{ads}$ , and, that the  $-2/3$  power law dependence suggestive of a diffusion process, we may hypothesize that the hydroxyl species, once formed, can diffuse across the surface. This would then mean that the formation of  $OH_{ads}$  on polycrystalline platinum in sulphuric acid, although fast and reversible at the initial adsorption sites must undergo a relatively slow diffusion process away from that initial site.

There are supporting arguments in the literature for this. Davies et al.<sup>63</sup> studied the oxidation of  $CO_{ads}$  on ruthenium modified Pt(111) and suggested that the second peak in the  $CO_{ads}$  oxidation transients was associated with the spill-over

and diffusion of the oxidant produced at the ruthenium sites via a surface Grotthus-like mechanism. In addition Neurock et al.<sup>50</sup> used DFT calculations to determine the overall reaction energies along with barriers for the activation of water and the oxidation of CO<sub>ads</sub> on Pt(111) and PtRu(111) surfaces. They stated that for potentials which are lower than or equal to the potential of zero charge, water activation is likely rate controlling. Of particular interest is that for the bifunctional mechanism where hydroxyl species are generated on Ru they proposed that the migration of surface hydroxyl intermediates on the Pt could occur via a low energy proton transfer path, instead of direct transfer of the OH<sub>ads</sub> species, similar to that suggested by Davies<sup>63</sup>, and Koper<sup>64</sup>. Indeed, the idea of hydrogen bonded water-OH<sub>ads</sub> network on a platinum surface has also been suggested by a number of other groups<sup>24, 65-71</sup>. Climent et al. use the proton-hopping Grotthus-like mechanism as the most likely explanation for the very significant increase of adsorption entropy with OH<sub>ads</sub> coverage<sup>24</sup>. And Wagner and Ross<sup>71</sup> reported that the anomalous features in the cyclic voltammetry of Pt(111) first seen by Clavilier et al. in 1979<sup>72</sup> are best explained by a hydrogen bonded aqueous network with an ability to transmit structural phase information over greater-than-molecular distances, caused by the partial oxidation of water clusters forming a hydrated OH<sub>ads</sub> layer, and that the presence of strongly adsorbing anions can disrupt this. Clavilier et al. later confirmed that this is the most likely explanation for the results they reported<sup>73</sup>. Therefore there does not appear to be any logical reason why this Grotthus-like mechanism could not apply on platinum surfaces without ruthenium. Interestingly, it is then possible to propose a mechanism for CO<sub>ads</sub> oxidation which does not rely on CO<sub>ads</sub> diffusion. The ideas presented by Markovic et al.<sup>7</sup> who discussed how mono-metallic surfaces can be both reducing and oxidising at the same potential can also help explain our results, which is an idea which is fundamental to the use of the potential of zero total charge as an alternative to the potential of zero charge<sup>38</sup>. Markovic et al.<sup>7</sup> explained that in alkaline solutions the remarkable effect of pH on the rate of CO<sub>ads</sub> oxidation on Pt was the pH dependent adsorption of OH<sub>ads</sub> at defect/step sites. In this paper we propose that the same effect should logically apply to acidic solutions, with the additional effect of anion adsorption<sup>39</sup> to explain the lower reactivity than expected compared to alkaline solutions<sup>74</sup>. We assume that our surface is inhomogeneous (which for polycrystalline Pt is necessary), and therefore at any potential at which we investigate, different regions will have different equilibrium coverages of OH<sub>ads</sub>. Then in order to achieve an equilibrium coverage of OH<sub>ads</sub> for the entire surface, we must consider the transfer of OH<sub>ads</sub> between these regions. The ability of surfaces to be both reducing and oxidising at the same potential is then crucial in understanding how the oxidation of CO<sub>ads</sub> occurs at low potentials, especially if one is concerned with real catalysts for fuel cell applications. Furthermore, we do not expect ideal single crystal electrode studies to exhibit this behaviour unless they have step edges or defects on the surface to simulate the inhomogeneities, such as those conducted by Lebedeva et al.<sup>12</sup>.

It might be expected that the current decay seen in the absence of adsorbed CO and the current decay seen in the presence of adsorbed CO are unrelated to each other and can be considered as parallel reactions. This would suggest that subtraction of the transients is a valid approach to extract the “CO-only” transient data. Indeed, as previously mentioned, this assumption has been utilised by several workers.

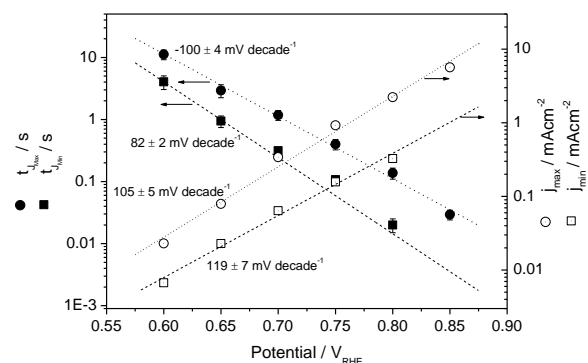


**Figure 6.** Time (closed symbols, left axis) and current density (open symbols, right axis) associated with the oxidation peak (●,○) and the minimum in current before the main CO<sub>ads</sub> oxidation peak (■,□) as a function of oxidation potential for saturated CO<sub>ads</sub> adlayers prepared by adsorption of CO at admission potentials of 50 mV, and an admission time of 10 s. The slopes and errors of the regression lines are shown in units of mV/decade. Data taken from Figure 3.

The results in Figure 3 (inset) suggest that this is not the case; especially at low potentials and that significant amounts of CO oxidation occur in the region commonly thought to be relatively unrelated to the CO oxidation process. As we will show below, there seems to be a strong coupling between the CO oxidation transient and the background transient seen in the absence of adsorbed CO.

### Transients in the presence of CO<sub>ads</sub>

Figure 6 presents the peak position and current density at the peak for the transients presented in Figure 3. It also provides the minimum current density seen before the CO oxidation peak. It was not possible to accurately resolve the peak position or current density at oxidation potentials above 850 mV, or minimum current density above 800 mV due to extremely rapid oxidation compared to the resolution of the experiment, or at oxidation potentials below 600 mV where both the timescales of the experiments were not sufficient and the noise was proportionally too great. For the potential range 600-850 mV both the oxidation peak time and the oxidation peak current density show an exponential response with potential. The slope of the regression lines for log peak current density versus potential is suggestive of a Tafel relationship with a transfer coefficient of approximately 0.38. We would expect a transfer coefficient of 0.5 for a completely reversible reaction, such as the reduction of water to OH<sub>ads</sub>. However, according to our hypothesis the peak in the CO<sub>ads</sub> oxidation reaction will be dependent upon the formation of the hydrogen bonded water-OH<sub>ads</sub> network and not the formation of OH<sub>ads</sub> directly.

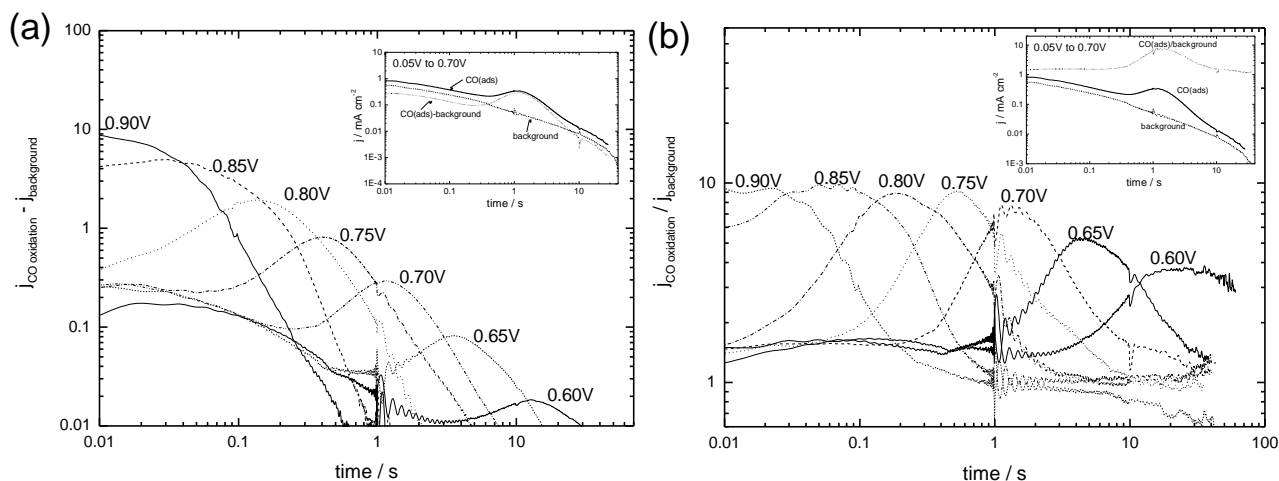


**Figure 7.** (a) The chrono-amperometric transients for the stripping of saturated  $\text{CO}_{\text{ads}}$  adlayers shown in Figure 3 subtracted by the chrono-amperometric transients in the absence of  $\text{CO}_{\text{ads}}$  shown in Figure 5. (b) The same transients but ratioed. Inset in each is an example of the process at 700 mV

5 The minimum before the peak in these transients clearly represents a point at which a change of mechanism occurs on the  $\text{CO}_{\text{ads}}$  oxidation reaction. Koper et al.<sup>53</sup> investigated the current densities in the plateau region on Pt(111) surfaces reported a Tafel slope of  $\sim 80 \text{ mV decade}^{-1}$  which would give a transfer coefficient of 0.26. It is not clear at what point Koper et al. measured the current for the plateau region. If they used the minimum (at different times) measured before the main  $\text{CO}_{\text{ads}}$  oxidation peak, which seems most likely, then by comparison our results shown in Figure 3 plotted as the current at the minimum are also shown in Figure 6 provide a Tafel slope of  $119 \pm 7 \text{ mV decade}^{-1}$  with a corresponding transfer coefficient of 0.5. This would be indicative of a completely reversible reaction, which is what we would expect for the dissociation of water to  $\text{OH}_{\text{ads}}$ . Therefore, although the formation of  $\text{OH}_{\text{ads}}$  at active sites can probably be considered as fast and reversible, the formation of a  $\text{OH}_{\text{ads}}$  adlayer on an inhomogeneous surface cannot. However, a direct comparison between our results and Koper's is not possible because of the polycrystalline nature of our surface, and for the reasons mentioned above this result should be treated with caution.

As described above, there seems to be a strong interaction between the “background” process occurring in the absence of CO and the CO oxidation process itself. We have seen this effect especially at low potentials where significant amounts of CO appear to be oxidised during the initial transient decay, Figure 3(inset). In order to understand the nature of this interaction we provide both the difference and ratio of the transients when a monolayer of CO is adsorbed on the surface and the background transient, Figure 7(a) and (b). This figure is produced from the data in Figure 3 and Figure 5. When we plot the difference in currents at each potential, Figure 7 (a), the resulting transients appear quite similar to those provided in Figure 3. The surprising result is when we calculate the ratio of the transients at each potential, Figure 7 (b). We obtain a set of transients which look surprisingly similar even though the potential range covered is 300mV – a much larger range than typically examined for such work. A number of

important features are seen in this transient

- 45 \* The peak current ratio remains constant for all of the potentials at which the majority of CO oxidation occurs in the peak (0.70-0.90). Over this same range of potentials, the absolute peak current density varies by more than a factor of 20 (Figure 3);
- 50 \* Before the oxidation peak, the ratio of currents shows a plateau of about 1.5x the background current in the absence of CO (as seen for the transients at 0.60-0.80 V).
  - \* After the oxidation peak the currents show a plateau close to 1;
- 55 \* The oxidation peaks are symmetrical with  $\log(\text{time})$  (see below for proof);
- \* The peaks have the same relative width and show a lognormal distribution;

Proof of the above assertions are shown in Figure 8 where the peaks are fit to a LogNormal distribution:

$$\frac{j_{\text{CO Oxidation}}}{j_{\text{Background}}} = \text{offset} + \frac{A}{\sqrt{2\pi} \times t \times \sigma} \text{Exp} \left( - \frac{\left( \log_e \left( \frac{t}{m} \right) \right)^2}{2\sigma^2} \right) \quad (4)$$

Where *offset* is the value which the transient asymptotically approaches at  $t \rightarrow 0$  and  $t \rightarrow \infty$ ; *A* is an amplitude factor and proportional to the height of the peak,  $\sigma$  the peak width (standard deviation of the peak) and *m* is a measure of the mean value of the transient. The peak current occurs at a value of  $m \exp(-\sigma^2)$ . The fits are surprisingly good, especially when one considers that the potential range covers 300mV, much larger than typically employed when fitting CO oxidation transients.

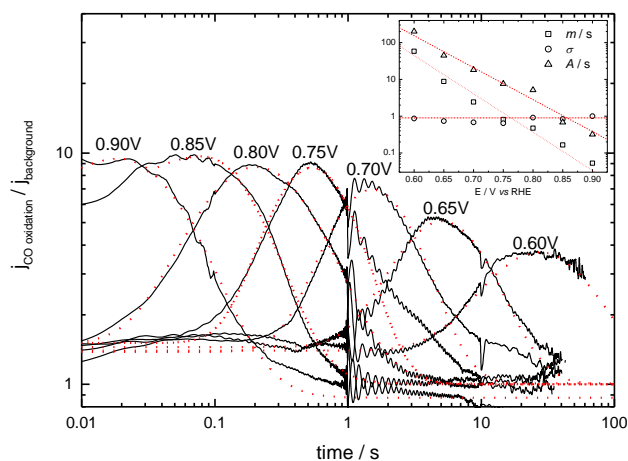


**Figure 8.** Transients provided in Figure 7(b) fit to the Lognormal distribution, Eqn 4. Inset shows the distribution of the fitting parameters with potential. In all cases the errors associated with the parameters are smaller than their corresponding symbols.

Inset into Figure 8 showing how the fitting parameters vary with potential. Error bars for the fitting parameters are smaller than the symbols on the graph and so have not been included. Of significant interest is that  $\sigma$ , a measure of the relative peak width remains more or less constant across the entire range of potentials. Furthermore, as previously identified, both of the other fitting parameters vary with a Tafel-like dependency with potential.

It is interesting that the peaks appear to follow a Log-Normal distribution. This distribution is typically seen when there are a large number of independent factors which multiplicatively combine. It is tempting to hypothesize that these independent factors are related to the large number of different crystal faces in the polycrystalline sample. Nonetheless, it is important to note that this is not an attempt to provide a model for the transients, rather we wish to highlight the statistically significant similarity between all of the peaks. In a future paper we will develop a model for these transients utilising a properly developed kinetic scheme.

The current transients in both the presence and absence of  $\text{CO}_{\text{ads}}$  when analysed in a log-log plot show a similarly shaped decay occurring over a potential range of 300 mV. In addition our results appear identical in feature with those obtained for  $\text{CO}_{\text{ads}}$  oxidation on Pt nanoparticles supported on glassy carbon in 0.1 mol  $\text{dm}^{-3}$   $\text{H}_2\text{SO}_4$ <sup>75</sup>; on Pt(111) surface in 0.1 mol  $\text{dm}^{-3}$   $\text{HClO}_4$ ,<sup>76</sup>; on a broad range of Pt single crystal surfaces in 0.5 mol  $\text{dm}^{-3}$   $\text{H}_2\text{SO}_4$ <sup>12</sup>; and also on mesoporous Pt catalyst in 0.5 mol  $\text{dm}^{-3}$   $\text{H}_2\text{SO}_4$ <sup>77</sup>, which suggests that our results are not peculiar to our experimental set-up or the use of polycrystalline Pt, but are instead a genuine phenomenon of Pt electrochemistry, and are therefore likely to be a property of the surface. The question again is how can a property of platinum surfaces affect  $\text{CO}_{\text{ads}}$  oxidation, and what is that property?

The simplest answer appears to be the formation of  $\text{OH}_{\text{ads}}$ . Therefore, we propose the following hypothetical mechanism: In the absence of  $\text{CO}_{\text{ads}}$ , upon stepping the potential a current decay is seen caused by double layer charging, the removal of  $\text{H}_{\text{ads}}$ , and the adsorption of anions and water, followed by the

formation of  $\text{OH}_{\text{ads}}$  at active sites. The continuing current is then the potential dependent formation of a hydrogen bonded water- $\text{OH}_{\text{ads}}$  network, growing from the active sites where the formation of  $\text{OH}_{\text{ads}}$  is fastest, slowed down by the displacement of anions. The long times taken to reach equilibrium is because although at higher potentials an adlayer of  $\text{OH}_{\text{ads}}$  is thermodynamically favourable over an adlayer of bisulphate anions, there is likely to be a considerable kinetic barrier to the displacement of the anions, and this must occur sequentially, spreading out from the active sites, to build up a hydrogen bonded water- $\text{OH}_{\text{ads}}$  network.

In the presence of a CO adlayer prepared in the hydrogen region and upon stepping the potential the initial large current is caused by double layer charging, the removal of  $\text{H}_{\text{ads}}$ , and some anion adsorption, followed by the formation of  $\text{OH}_{\text{ads}}$  at active sites. Both anion and water adsorption occur as the CO adlayer is removed, as does some reorganisation of the adlayer. During this period the predominant current is the formation of  $\text{OH}_{\text{ads}}$  at active sites, followed by the diffusion of the  $\text{OH}_{\text{ads}}$  to the  $\text{CO}_{\text{ads}}$  boundary. The limiting factor in the process is the potential dependent formation of a hydrogen bonded water- $\text{OH}_{\text{ads}}$  network; growing from the active sites where the formation of  $\text{OH}_{\text{ads}}$  is fastest, slowed down by the displacement of anions. This leads to a surface diffusion limitation in provision of  $\text{OH}_{\text{ads}}$ . Removal of  $\text{OH}_{\text{ads}}$  by reaction with CO accelerates the production of  $\text{OH}_{\text{ads}}$ . At higher potentials both the formation of  $\text{OH}_{\text{ads}}$  and the displacement of bisulphate anions will occur more readily. A critical supporting piece of evidence for this hypothesis is that independent of oxidation potential, the current observed in the presence of a CO adlayer is higher by the same amount (50%) than that seen in the absence of a CO adlayer, (e.g. see Figure 7(b) inset). It would seem that the CO oxidation reaction occurring before the main peak is directly associated with the transient seen in the absence of CO. However, the surfaces in the presence and absence of CO are very different, hence highlighting the effect of a relatively small number of highly active sites which function under both conditions to produce  $\text{OH}_{\text{ads}}$ .

### CO reorganisation compared to $\text{OH}_{\text{ads}}$ redistribution

To summarise briefly, the early onset of  $\text{CO}_{\text{ads}}$  oxidation is now widely acknowledged as being caused by a competitive adsorption between hydrogen and CO when CO is admitted at potentials within the hydrogen region (<350 mV)<sup>9, 42-47</sup>. Upon polarisation to higher potentials, oxidative removal of the adsorbed hydrogen forms many small CO free regions distributed throughout the  $\text{CO}_{\text{ads}}$  adlayer. These CO free regions then allow the adsorption and/or formation of oxygen containing species, which react with the  $\text{CO}_{\text{ads}}$  to form  $\text{CO}_2$ . The species involved in the initial reaction with  $\text{CO}_{\text{ads}}$  is generally regarded to be  $\text{OH}_{\text{ads}}$  formed by the dissociation of adsorbed water<sup>1, 6, 15-17, 29, 35, 48-50</sup>. L-H kinetics are often written such that there is an implicit assumption that any free sites formed in the adlayer will promote the formation of  $\text{OH}_{\text{ads}}$  through rapid spontaneous dissociative oxidative adsorption of bulk water<sup>2, 12, 51-55</sup>. In addition although the presence of a  $\text{COOH}_{\text{ads}}$  intermediate has been reported<sup>3-5, 12,</sup>

49, 50, 78, 79, it is often considered to be so transient that it is not important<sup>5</sup>. The third step in the oxidation of CO<sub>ads</sub> is generally ignored and assumed to be extremely fast compared to the first and second, and is implicitly assumed to be via reaction with bulk water to form H<sub>3</sub>O<sup>+</sup><sup>5, 49, 80</sup>. Whether COOH<sub>ads</sub> is adsorbed onto one or two sites is highly dependent upon potential, at lower potentials it will adsorb through both the C and H atoms whereas at higher potentials it will form a Pt-CO<sub>2</sub><sup>δ-</sup>-H<sup>δ+</sup> state stabilised by the solution<sup>50</sup>. It should be noted that this is still likely to sterically hinder any available sites adjacent to it, and so can reasonably be considered to occupy 2 sites in both cases. At high potentials this consideration is negligible, but this may be important at low potentials (<500 mV).

15 If the diffusion of either of the species on the surface is assumed to be relatively fast then the reaction can be modelled as proportional to the coverage of CO<sub>ads</sub> and OH<sub>ads</sub> known as the mean field approximation. For this approximation when OH<sub>ads</sub> formation is assumed to be fast the rate of reaction is then relative to the rate of formation of OH<sub>ads</sub><sup>54, 79</sup>, which is effectively equal to the number of free sites, coupled with the effective diffusion rate of the CO<sub>ads</sub><sup>2, 12, 75, 76, 80-84</sup>, any segregation of adsorbed species that may occur<sup>85, 86</sup>, and any effect of the redistribution or reorganisation of the CO<sub>ads</sub> adlayer during oxidation<sup>9, 12, 40, 42, 78, 80, 87</sup>.

However the mean field approximation is misleading as it assumes that OH<sub>ads</sub> will be formed spontaneously upon the adsorption of water, which is unlikely except at very high potentials (>800 mV). In addition the role of the adsorption of water and anions cannot be overlooked<sup>71</sup>, and their role in forming or suppressing the formation of a hydrogen bonded water-OH<sub>ads</sub> network appears to be crucial in understanding the CO<sub>ads</sub> oxidation process<sup>24, 65-71</sup>.

35 Both Bergelin et al.<sup>80</sup> and Koper et al.<sup>53</sup> invoked a reorganisation mechanism to explain the initial current plateau that they observed, where the initial oxidation of CO<sub>ads</sub> is accompanied by a reorganisation or redistribution of the adlayer such that there is no effective freeing of sites, and as the oxidation proceeds the ability of this reorganisation mechanism to compensate for the removal of CO<sub>ads</sub> decreases due to the CO<sub>ads</sub> adlayer becoming more stable. Therefore at some critical point the rate of CO<sub>ads</sub> oxidation overtakes the rate of reorganisation and it is at this point that the L-H mean-field mechanism is initiated. This mechanism is theoretically plausible and as reported by Markovic et al.<sup>11</sup> it is possible to observe this reorganisation phenomenon on Pt(111) and as we will present in a further paper it is also possible to observe it on polycrystalline platinum<sup>88</sup>. A key point to note is that this mechanism will only work using conventional models if the CO oxidation at the initial sites is proceeding fast enough such that the reorganisation mechanism is incapable of covering over these sites, as otherwise after the initial activation of the surface, the reorganisation mechanism would be expected to compensate totally and shut down oxidation entirely, forming a completely stable CO<sub>ads</sub> adlayer.

From Figure 3 we can see that the so-called “current plateau” is in fact an interaction of the background decay with the

slowly rising edge of the CO<sub>ads</sub> oxidation peak. However, this decay is only really visible in a log-time plot, as otherwise the eye is ‘misled’ into seeing a plateau, especially if one presents CO oxidation transients from which a background transient has been subtracted. The currents seen during the initial part of the transient appear to be only marginally dependent upon the potential with the only parameter significantly dependent upon potential being the time taken before the onset of the main CO<sub>ads</sub> oxidation peak. This is hard to explain using conventional models. The main CO<sub>ads</sub> oxidation peak then appears to follow standard L-H kinetics with a Tafel slope of 105±5 mV/decade for the peak current density as shown in Figure 6. It is important that the initial rate of CO<sub>ads</sub> oxidation with a slow decay can only be explained if a constant current at the active sites is assumed, with a diffusion limited process inhibiting the reaction between OH<sub>ads</sub> from the active sites and CO<sub>ads</sub>. This could be either diffusion of CO<sub>ads</sub> to the active sites or diffusion of OH<sub>ads</sub> from the active sites. That the chrono-amperometric transients in the absence of an adlayer of CO<sub>ads</sub> are broadly identical to those in the presence of an adlayer of CO<sub>ads</sub> except for the main CO<sub>ads</sub> oxidation peak, suggests that the limiting diffusion process occurs in both transients. Therefore, it cannot be the diffusion of CO<sub>ads</sub> (since CO is not present in the background transients), and therefore must be diffusion of OH<sub>ads</sub> from the active sites. The peak in the chrono-amperometric transients shown in Figure 3 actually represents the reaction of OH<sub>ads</sub> with CO<sub>ads</sub> to produce COOH<sub>ads</sub> which rapidly reacts to form CO<sub>2</sub>, H<sup>+</sup> and e<sup>-</sup>. As OH<sub>ads</sub> is removed from the system it is rapidly replaced, giving rise to a peak which is effectively limited by the chemical reaction between CO<sub>ads</sub> and OH<sub>ads</sub>.

90 At high potentials (>700 mV) the simplification used in the mean-field approximation can give reasonable fits to the main CO<sub>ads</sub> oxidation peak (although those fits typically ignore any additional currents seen during CO<sub>ads</sub> oxidation), but at lower potentials this simplification will no longer work. Hence it might be expected that a change in reaction mechanism should be observed. For our results, there does not appear to be any change in mechanism down to at least 600mV, as we see a consistent change in peak size, shape position and properties. In addition, the observation that active sites play a particularly important role in the CO<sub>ads</sub> oxidation reaction at low potentials<sup>12, 89</sup> cannot be reconciled using the mean-field approximation described here. Instead there must be different rates for the formation of OH<sub>ads</sub> on the active sites, such that the formation of OH<sub>ads</sub> at the active sites is faster than on the plateaux. The reaction can then best be explained by the OH<sub>ads</sub> spill over mechanism suggested by Hayden et al. for PtRu<sup>63</sup> forming a hydrogen bonded water-OH<sub>ads</sub> network. This can also explain the current decay seen before the main CO<sub>ads</sub> oxidation peak.

110 Figure 4 shows how the peak in the CO<sub>ads</sub> oxidation transient does not correspond to a relative coverage of 0.5, but decreases significantly with potential, as might be expected if the OH<sub>ads</sub> coverage has a strong potential dependence. The onset of the main CO<sub>ads</sub> oxidation peak then corresponds to the point at which the formation of OH<sub>ads</sub> within the CO<sub>ads</sub> free region becomes comparable to and/or overtakes the

formation and diffusion of  $\text{OH}_{\text{ads}}$  from the active sites. Thus the main  $\text{CO}_{\text{ads}}$  oxidation peak current decreases exponentially and the peak time increases exponentially with decreasing potential. This is directly related to the equilibrium coverage of  $\text{OH}_{\text{ads}}$  within the hydrogen bonded water- $\text{OH}_{\text{ads}}$  network; hence the Tafel slopes for both reflect the rate determining step, which is the production of  $\text{OH}_{\text{ads}}$ . At very low potentials the reaction can theoretically proceed until completion via the formation and diffusion of  $\text{OH}_{\text{ads}}$  from the active sites, as even on a completely  $\text{CO}_{\text{ads}}$  free surface the equilibrium coverage of  $\text{OH}_{\text{ads}}$  will be negligible. This can be seen in Figure 4(inset). If this model is correct then there should be no  $\text{CO}_{\text{ads}}$  oxidation peak below the potential of zero total charge for the surface. By extrapolating the potential below which no  $\text{CO}_{\text{ads}}$  oxidation peak should occur from the linear fit shown in Figure 4(inset) a potential of  $280 \pm 130$  mV is estimated, which is consistent with the potential of zero charge of  $234 \pm 5$  mV which we measured for our surface. This is also consistent with extrapolation of the integrated peak charges observed in the plot inset into Figure 3. Therefore we could assume that there are two regions of the  $\text{CO}_{\text{ads}}$  oxidation process, the first occurring during the current decay and the second during the peak. It is striking that the peaks seem to follow a log-normal distribution – i.e. the rate of oxidation follows  $\log(\text{time})$  behaviour. This type of response is somewhat different from nucleation and growth type-models, and certainly not expected from a pure mean-field model in which surface transport is not a limiting process. A mathematical model for this process will be presented in a future paper.

## Conclusion

One of the characteristic features of chronoamperometric  $\text{CO}_{\text{ads}}$  oxidation transients, often reported in the literature, is their high degree of asymmetry. Contrary to this prevailing view we have shown in this paper that the peaks appear symmetrical – but in  $\log(t)$ , not  $t$ . We also see that the CO oxidation process seems to be intimately linked to the production of  $\text{OH}_{\text{ads}}$  on the surface, and that over the potential range studied,  $\text{OH}_{\text{ads}}$  diffusion may be a rate limiting process. On these polycrystalline surfaces it would appear that it is the formation and diffusion of  $\text{OH}_{\text{ads}}$  across the surface which limits the rate of  $\text{CO}_{\text{ads}}$  oxidation. This diffusion mechanism is intimately related to the formation of a hydrogen bonded water- $\text{OH}_{\text{ads}}$  network, in acidic solutions complicated by the presence of strongly adsorbing anions. We suggest that the main  $\text{CO}_{\text{ads}}$  oxidation peak reflects the point at which the potential dependent equilibrium coverage of  $\text{OH}_{\text{ads}}$  within the hydrogen bonded water- $\text{OH}_{\text{ads}}$  network is sufficiently high that the rate of formation of  $\text{OH}_{\text{ads}}$  within this network approaches the rate of formation at the active sites. In this paper we cannot fully explain the intricacies of this mechanism, but believe the hypothetical model presented in this paper is capable of explaining the electrochemical oxidation of  $\text{CO}_{\text{ads}}$  on platinum in all the papers reported. We contend that in the absence of  $\text{CO}_{\text{ads}}$  stepping the potential will also give rise to measurable currents over extended timescales, and these are also a result of the formation and

diffusion of  $\text{OH}_{\text{ads}}$  across the surface, establishing a new equilibrium hydrogen bonded water- $\text{OH}_{\text{ads}}$  network, and the extended timescales are likely to be caused by the presence of strongly adsorbed anions. Therefore, we suggest that the underlying process giving rise to the currents measured when stepping potential in both the presence and absence of  $\text{CO}_{\text{ads}}$  adlayers on polycrystalline platinum is the formation of a hydrogen bonded water- $\text{OH}_{\text{ads}}$  network, slowed down by the displacement of anions, and this process is the rate determining step in the  $\text{CO}_{\text{ads}}$  oxidation mechanism. This process is seen as a power law decay in the transients in the presence and absence of  $\text{CO}_{\text{ads}}$ . Although the formation of  $\text{OH}_{\text{ads}}$  is fast on ideal single crystals surfaces in the absence of strongly adsorbing anions, it seems that on polycrystalline platinum or nanoparticles of platinum, this process may be fast only on certain sites, and so it takes some time for the surface to equilibrate. It may be useful to revise the assumption of fast  $\text{OH}_{\text{ads}}$  production in  $\text{CO}_{\text{ads}}$  oxidation models which are applied to real fuel cell systems.

## Acknowledgements

The authors would like to thank Dr. Alan Palmer for his invaluable assistance when using the impinging jet, and Stephen Atkins for his help in building much of the apparatus.

## References

1. L. D. Burke, *Electrochim. Acta*, 1994, **39**, 1841-1848.
2. M. T. M. Koper, A. P. J. Jansen, R. A. van Santen, J. J. Lukkier and P. A. J. Hilbers, *J. Chem. Phys.*, 1998, **109**, 6051-6062.
3. B. D. Dunietz, N. M. Markovic, P. N. Ross and M. Head-Gordon, *J. Phys. Chem. B*, 2004, **108**, 9888-9892.
4. J. Narayanasamy and A. B. Anderson, *J. Electroanal. Chem.*, 2003, **554**, 35-40.
5. T. E. Shubina, C. Hartnig and M. T. M. Koper, *Phys. Chem. Chem. Phys.*, 2004, **6**, 4215-4221.
6. B. N. Grgur, N. M. Markovic, C. A. Lucas and P. N. Ross, *Journal of the Serbian Chemical Society*, 2001, **66**, 785-797.
7. N. M. Markovic and J. Ross, P. N., *Surf. Sci. Rep.*, 2002, **45**, 117-229.
8. Z. Jusys, J. Kaiser and R. J. Behm, *Phys. Chem. Chem. Phys.*, 2001, **3**, 4650-4660.
9. R. Ianniello, V. M. Schmidt, U. Stimming, J. Stumper and A. Wallau, *Electrochim. Acta*, 1994, **39**, 1863-1869.
10. W. G. Golden, K. Kunimatsu and H. Seki, *J. Phys. Chem.*, 1984, **88**, 1275.
11. N. M. Markovic, B. N. Grgur, C. A. Lucas and P. N. Ross, *J. Phys. Chem. B*, 1999, **103**, 487-495.
12. N. P. Lebedeva, M. T. M. Koper, J. M. Feliu and R. A. van Santen, *J. Phys. Chem. B*, 2002, **106**, 12938-12947.
13. L. D. Burke and A. J. Ahern, *J. Solid State Electrochem.*, 2001, **5**, 553-561.
14. S. A. Bilmes and A. J. Arvia, *J. Electroanal. Chem.*, 1993, **361**, 159-167.
15. S. A. Bilmes, N. Giordano and A. J. Arvia, *Canadian Journal of Chemistry*, 1988, **66(9)**, 2259.

16. A. N. Frumkin, O. Petrii and T. Kolotyrkina-Safonova, *Dokl. Akad. Nauk SSSR*, 1975, **222**, 1159.
17. J. O. M. Bockris, S. D. Argade and E. Gileadi, *Electrochim. Acta*, 1969, **14**, 1259.
18. B. E. Conway, B. Barnett, H. Angersteinkozłowska and B. V. Tilak, *J. Chem. Phys.*, 1990, **93**, 8361-8373.
19. H. Angersteinkozłowska, B. E. Conway, K. Tellefsen and B. Barnett, *Electrochim. Acta*, 1989, **34**, 1045-1056.
20. M. E. van der Geest, N. J. Dangerfield and D. A. Harrington, *J. Electroanal. Chem.*, 1997, **420**, 89-100.
21. M. Alsabet, M. Grden and G. Jerkiewicz, *J. Electroanal. Chem.*, 2006, **589**, 120-127.
22. Angerste.H, B. E. Conway and W. B. A. Sharp, *J. Electroanal. Chem.*, 1973, **43**, 9-36.
23. G. Jerkiewicz, G. Vatankhah, J. Lessard, M. P. Soriaga and Y. S. Park, *Electrochim. Acta*, 2004, **49**, 1451-1459.
24. V. Climent, R. Gomez, J. M. Orts and J. M. Feliu, *J. Phys. Chem. B*, 2006, **110**, 11344-11351.
25. B. E. Conway, *Progress in Surface Science*, 1995, **49**, 331-452.
26. C. McCallum and D. Pletcher, *J. Electroanal. Chem.*, 1976, **70**, 277-290.
27. L. A. Kibler, A. Cuesta, M. Kleinert and D. M. Kolb, *J. Electroanal. Chem.*, 2000, **484**, 73-82.
28. B. A. Boukamp, *J. Electrochem. Soc.*, 1995, **142**, 1885-1894.
29. T. Iwasita and X. H. Xia, *J. Electroanal. Chem.*, 1996, **411**, 95-102.
30. J. Clavilier, *J. Electroanal. Chem.*, 1980, **107**, 211-216.
31. N. M. Markovic, T. J. Schmidt, B. N. Grgur, H. A. Gasteiger, R. J. Behm and P. N. Ross, *J. Phys. Chem. B*, 1999, **103**, 8568-8577.
32. N. S. Marinkovic, N. M. Markovic and R. R. Adzic, *J. Electroanal. Chem.*, 1992, **330**, 433-452.
33. A. Kolics and A. Wieckowski, *J. Phys. Chem. B*, 2001, **105**, 2588-2595.
34. K. Yamamoto, D. M. Kolb, R. Kotz and G. Lehmpfuhl, *J. Electroanal. Chem.*, 1979, **96**, 233-239.
35. K. J. J. Mayrhofer, B. B. Blizanac, M. Arenz, V. R. Stamenkovic, P. N. Ross and N. M. Markovic, *J. Phys. Chem. B*, 2005, **109**, 14433-14440.
36. G. A. Attard, O. Hazzazi, P. B. Wells, V. Climent, E. Herrero and J. M. Feliu, *J. Electroanal. Chem.*, 2004, **568**, 329-342.
37. V. Climent, R. Gomez, J. M. Orts, A. Rodes, A. Aldaz and J. M. Feliu, Marcel Dekker, New York, 1999, p. 463.
38. K. J. J. Mayrhofer, M. Arenz, B. B. Blizanac, V. Stamenkovic, P. N. Ross and N. M. Markovic, *Electrochim. Acta*, 2005, **50**, 5144-5154.
39. M. Arenz, K. J. J. Mayrhofer, V. Stamenkovic, B. B. Blizanac, T. Tomoyuki, P. N. Ross and N. M. Markovic, *J. Am. Chem. Soc.*, 2005, **127**, 6819-6829.
40. K. Kunimatsu, H. Seki, W. G. Golden, J. G. Gordon and M. R. Philpott, *Langmuir*, 1986, **2**, 464-468.
41. J. A. Caram and C. Gutierrez, *J. Electroanal. Chem.*, 1991, **305**, 259-274.
42. A. Lopez-Cudero, A. Cuesta and C. Gutierrez, *J. Electroanal. Chem.*, 2005, **579**, 1-12.
43. A. Rincon, M. C. Perez, A. Cuesta and C. Gutierrez, *Electrochem. Commun.*, 2005, **7**, 1027-1032.
44. C. S. Kim, C. Korzeniewski and W. J. Tornquist, *J. Chem. Phys.*, 1994, **100**, 628-630.
45. H. Kita, S. Ye and K. Sugimura, *J. Electroanal. Chem.*, 1991, **297**, 283-296.
46. L. Grambow and S. Bruckenstein, *Electrochim. Acta*, 1977, **22**, 377-383.
47. E. P. M. Leiva, E. Santos and T. Iwasita, *J. Electroanal. Chem.*, 1986, **215**, 357-367.
48. L. D. Burke, M. A. Horgan, L. M. Hurley, L. C. Nagle and A. P. O'Mullane, *J. Appl. Electrochem.*, 2001, **31**, 729-738.
49. E. Herrero, B. Alvarez, J. M. Feliu, S. Blais, Z. Radovic-Hrapovic and G. Jerkiewicz, *J. Electroanal. Chem.*, 2004, **567**, 139-149.
50. S. Desai and M. Neurock, *Electrochim. Acta*, 2003, **48**, 3759-3773.
51. M. T. M. Koper, N. P. Lebedeva and C. G. M. Hermse, *Faraday Discuss.*, 2002, **121**, 301-311.
52. B. Love and J. Lipkowski, in *Molecular Phenomena at Electrode Surfaces*, ed. M. Soriaga, ACS Symp Ser, 1988, pp. 484-496.
53. N. P. Lebedeva, M. T. M. Koper, J. M. Feliu and R. A. van Santen, *J. Electroanal. Chem.*, 2002, **524**, 242-251.
54. D. C. Azevedo, A. L. N. Pinheiro, R. M. Torresi and E. R. Gonzalez, *J. Electroanal. Chem.*, 2002, **532**, 43-48.
55. S. Gilman, *The Journal of Physical Chemistry*, 1964, **68**, 70-80.
56. T. Kobayashi, P. K. Babu, J. H. Chung, E. Oldfield and A. Wieckowski, *Journal of Physical Chemistry C*, 2007, **111**, 7078-7083.
57. M. Bergelin and M. Wasberg, *J. Electroanal. Chem.*, 1998, **449**, 181-191.
58. C. L. Green and A. Kucernak, *J. Phys. Chem. B*, 2002, **106**, 1036-1047.
59. G. J. Offer and A. Kucernak, *J. Electroanal. Chem.*, 2008, **613**, 171-185.
60. J. L. Melville, B. A. Coles, R. G. Compton, N. Simjee, J. V. Macpherson and P. R. Unwin, *J. Phys. Chem. B*, 2003, **107**, 379-386.
61. A. Rodes, J. M. Orts, J. M. Perez, J. M. Feliu and A. Aldaz, *Electrochem. Commun.*, 2003, **5**, 56-60.
62. V. Stamenkovic, K. C. Chou, G. A. Somorjai, P. N. Ross and N. M. Markovic, *J. Phys. Chem. B*, 2005, **109**, 678-680.
63. J. C. Davies, B. E. Hayden, D. J. Pegg and M. E. Rendall, *Surf. Sci.*, 2002, **496**, 110-120.
64. P. Vassilev, M. T. M. Koper and R. A. van Santen, *Chem. Phys. Lett.*, 2002, **359**, 337-342.
65. P. Vassilev, M. J. Louwerse and E. J. Baerends, *Chem. Phys. Lett.*, 2004, **398**, 212-216.
66. G. S. Karlberg and G. Wahnstrom, *Physical Review Letters*, 2004, **92**.
67. C. Clay, S. Haq and A. Hodgson, *Physical Review Letters*, 2004, **92**.
68. A. P. Seitsonen, Y. J. Zhu, K. Bedurftig and H. Over, *J. Am. Chem. Soc.*, 2001, **123**, 7347-7351.
69. A. Michaelides and P. Hu, *J. Chem. Phys.*, 2001, **114**, 513-519.

- 
70. K. Bedürftig, S. Volkening, Y. Wang, J. Wintterlin, K. Jacobi and G. Ertl, *J. Chem. Phys.*, 1999, **111**, 11147-11154.
71. F. T. Wagner and P. N. Ross, *J. Electroanal. Chem.*, 1988, **250**, 301-320.
- 5 72. J. Clavilier, R. Faure, G. Guinet and R. Durand, *J. Electroanal. Chem.*, 1979, **107**, 205-209.
73. V. Lazarescu and J. Clavilier, *Electrochim. Acta*, 1998, **44**, 931-941.
74. J. S. Spendelow, G. Q. Lu, P. J. A. Kenis and A. Wieckowski, *J. Electroanal. Chem.*, 2004, **568**, 215-224.
- 10 75. O. V. Cherstiouk, P. A. Simonov, V. I. Zaikovskii and E. R. Savinova, *J. Electroanal. Chem.*, 2003, **554**, 241-251.
76. A. V. Petukhov, W. Akemann, K. A. Friedrich and U. Stimming, *Surf. Sci.*, 1998, **404**, 182-186.
- 15 77. J. H. Jiang and A. Kucernak, *J. Electroanal. Chem.*, 2002, **533**, 153-165.
78. Y. M. Zhu, H. Uchida and M. Watanabe, *Langmuir*, 1999, **15**, 8757-8764.
79. A. B. Anderson and N. M. Neshev, *J. Electrochem. Soc.*, 2002, **149**, E383-E388.
- 20 80. M. Bergelin, E. Herrero, J. M. Feliu and M. Wasberg, *J. Electroanal. Chem.*, 1999, **467**, 74-84.
81. N. M. Markovic, B. N. Grgur, C. A. Lucas and P. N. Ross, *Surf. Sci.*, 1997, **384**, L805-L814.
- 25 82. F. Maillard, M. Eikerling, O. V. Cherstiouk, S. Schreier, E. Savinova and U. Stimming, *Faraday Discuss.*, 2004, **125**, 357-377.
83. F. Maillard, S. Schreier, M. Hanzlik, E. R. Savinova, S. Weinkauff and U. Stimming, *Phys. Chem. Chem. Phys.*, 2005, **7**, 385-393.
- 30 84. F. Maillard, E. R. Savinova, P. A. Simonov, V. I. Zaikovskii and U. Stimming, *J. Phys. Chem. B*, 2004, **108**, 17893-17904.
85. M. W. Severson and M. J. Weaver, *Langmuir*, 1998, **14**, 5603-5611.
- 35 86. V. P. Zhdanov and B. Kasemo, *Surf. Sci.*, 2003, **545**, 109-121.
87. I. Oda, J. Inukai and M. Ito, *Chem. Phys. Lett.*, 1993, **203**, 99-103.
88. G. J. Offer, in *Department of Chemistry, PhD Thesis*, Imperial College London, UK, 2007, p. 287.
- 40 89. N. P. Lebedeva, A. Rodes, J. M. Feliu, M. T. M. Koper and R. A. van Santen, *J. Phys. Chem. B*, 2002, **106**, 9863-9872.